Parameter Evaluation for Microwave Undulator Schemes

M. Seidel

April 10, 2001

Abstract

An undulator can be realized not only by static magnetic fields, but also by an electromagnetic wave in a waveguide. The major advantage is fast tunability of the RF undulator, whereas on the downside the field strength seems to be limited at levels of $0.2 \ldots 0.3\,\mathrm{T}$. In this note different schemes, involving rectangular and circular waveguides, are being investigated. Achievable field levels, required RF power, tolerances, helical polarization and pro's and con's of such schemes are discussed quantitatively. A practical test of an S-band normalconducting RF undulator is imaginable in the TESLA test facility. Available S-band klystrons could be used for the experiment.

1 Principles

An electromagnetic wave in a waveguide can impose alternating forces on a charged particle that travels through the guide. This principle can be used to realize a microwave undulator. It was demonstrated experimentally by Shintake and colleagues in 1983 [1]. Practically useful are TE modes which impose transverse deflections on the beam and do not interact longitudinally. The lowest modes are the TE_{10} mode for rectangular waveguides and TE_{11} for circular ones. The force on the speed-of-light particle is the sum of a magnetic and an electric component:

$$\begin{aligned}
\vec{F} &= e(\vec{E} + \vec{v} \times \vec{B}) = e(E_x - cB_y)\vec{e_x} \\
F_x &= \frac{e\hat{E}}{c}\left(1 \pm \sqrt{1 - \omega_c^2/\omega^2}\right)\sin(\omega t \pm k_g z) \qquad (1)
\end{aligned}$$

Here $\hat{E}$ is the peak E field on the waveguide axis, ω_c is the cutoff frequency of the considered mode and ω is the operating frequency which should be higher than the cutoff frequency, but lower than the frequency of the next possible mode. The $\pm$ sign holds for a wave that runs either with ($-$, forward) or against ($+$, backward) the beam direction. The guide wavenumber is $k_g = \sqrt{\omega^2 - \omega_c^2}/c$. The effective wavelength of the microwave undulator is derived as follows:

$$\begin{aligned}
z(t) &= ct \\
\omega t \pm k_g z &= (k \pm k_g)z = k_u z \\
\lambda_u &= \frac{\lambda \lambda_g}{\lambda_g \pm \lambda} = \frac{\lambda}{1 \pm \sqrt{1 - \omega_c^2/\omega^2}} \qquad (2)
\end{aligned}$$

Here λ is the free space wavelength and λ_u the equivalent undulator wavelength. Derivations of the analytically calculable field distributions for rectangular and circular waveguides are found in the Appendix of this paper. As we see from (1) the force can be significantly stronger for a backward wave. The effective wavelength of the backward traveling wave is shorter by up to a factor 2 as compared to the free space wavelength. In [1] a standing wave cavity has been used. A standing wave is composed by equal parts from a forward and a backward wave. For a high ratio ω/ω_c the microwave power flowing in the forward direction is practically lost for the undulator effect, nevertheless it fully contributes to the performance limiting peak field levels on the waveguide surface. Furthermore it turns out that the long wavelength force, originated by the forward part of the wave, leads to large orbit excursions of the beam [2]. For these reasons we conclude that a pure backward wave is better suited for a microwave undulator.

The equivalent undulator field strength scales with the square-root of the traveling microwave power, and proportional to the frequency (or inversely proportional to the waveguide dimension). The maximum undulator field is limited by the following two issues: 1.) The maximum microwave power that can be made available to the waveguide. 2.) The maximum field levels that can be accepted on the walls of the waveguide. Concerning the second point one has to distinguish furthermore normalconducting waveguide, were the electrical breakdown field is a concern, and superconducting waveguide with a usually earlier limitation in the maximum magnetic field on the surface. Both points will be discussed below in some detail.

Rectangular waveguide is the simplest choice for a planer undulator. The dimensions are normally chosen such that only the fundamental mode can be excited. The undulator wavelength is determined by the longer of the two guide dimensions a. The shorter dimension b can be tapered to compensate RF losses along the guide (if tolerances require this). In a quadratic waveguide two modes, of horizontal and vertical polarization, can be excited with equal phase velocity. If the phase difference is $90°$ this generates a helically polarized wave. The beam sees a rotating effective field with constant magnitude. The radiated power is doubled while the surface field levels in the guide stay the same as for the single mode undulator.

In a circular waveguide the ratio of undulator field to surface field is higher. Also a round waveguide allows to realize a helical undulator by exciting two TE_{11} modes at the same frequency in phase and space quadrature. The problem with circular guide is that the orientation of the TE_{11} mode is very sensitive to small deviations from the ideal circular shape of the guide.

2 Resonant Ring

A basic property of the microwave undulator is the fact that no energy is transferred from the electromagnetic field to the beam. The undulator radiation eats up only the kinetic energy of the beam. Therefore one can use a high Q resonant arrangement to amplify moderate levels of microwave input power by a large factor, limited only by the power dissipated in the guide walls. The simplest resonant arrangement is a closed standing wave cavity, possibly superconducting. However, as discussed in section 1 this has the unavoidable disadvantage of a forward wave component at the cost of a factor 2 in maximum field strength. A resonant ring or traveling wave resonator (TWR) is a closed waveguide ring which is weekly coupled to a microwave source via a directional coupler (Fig. 1).

The principle can be explained as follows. The field level in the ring, behind the coupler, is a superposition of input field from the source and circulating field at the other end of the coupler. This equation can be solved for the circulating field in the ring:

$$E_c \quad = \quad icE_i + \eta\sqrt{1-c^2}E_c$$

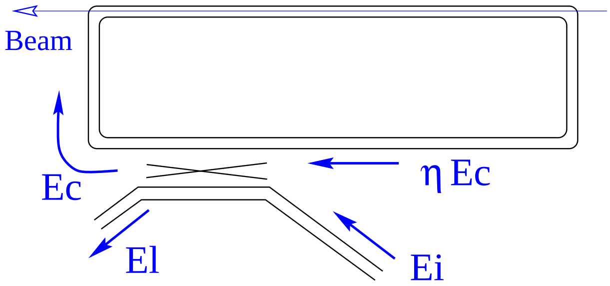

Figure 1: Principle of a resonant ring as microwave undulator.

$$E_c \;=\; \frac{ic}{1-\eta\sqrt{1-c^2}}E_i$$

Here c is the voltage coupling factor of the coupler and η is the voltage attenuation around the ring. The connection of η with the waveguide attenuation factor α, as derived in the Appendix, is: $\eta = \exp(-\alpha L)$, were L is the ring length. The circulating field can be maximized by a proper choice of the coupling factor $c_{\text{opt}} = \sqrt{1-\eta^2}$. The maximum achievable circulating field and power are then:

$$\begin{aligned} E_c^{\text{opt}} &= \frac{i}{\sqrt{1-\eta^2}}E_i \\ P_c^{\text{opt}} &= \frac{1}{1-\eta^2}P_i \;\approx\; \frac{1}{2\alpha L}P_i \end{aligned} \tag{3}$$

In order to obtain high circulating power levels the attenuation in the waveguide should be as small as possible. The attenuation constant α is proportional to the surface resistance R_s of the guide material. Copper is a good choice and at room temperature it has a surface resistance of: $R_s(\text{Cu})[\Omega] = 8.2 \cdot 10^{-3}\sqrt{f[\text{GHz}]}$. Further improvement can be achieved by cooling a copper waveguide to liquid nitrogen, or even helium temperatures to lower the attenuation. Unfortunately the gain is not very big since the surface resistance scales with the square root of the resistivity. In addition the gain is reduced by the anomalous skin effect. Following Padamse [3] one can expect an improvement factor 3 at 80 K and a factor 6 at 4 K. The DC conductivity is improved by much larger factors at the same temperatures. A real significant improvement can be achieved by using superconducting waveguides. For example layers of sputtered Nb_3Sn at 4.5 K, 3.0 GHz can have an R_s of 500 nΩ [4], bulk Nb at 1.8 K has about 15 nΩ. Fig. 2 summarizes different material and temperature options. It shows the theoretically achievable power amplification factor in resonant rings of rectangular waveguide as a function of ring length.

3 Maximum Surface Field and Numerical Examples

Achievable field levels in a normalconducting TWR are limited by the breakdown electrical field on the copper surface. As an example of present state of the art devices one can cite a resonant ring at SLAC, X-band [6], as listed in table 1, **first example**. This ring is operated with up to 300 MW circulating power at an input power of 30 MW. The ring was never intended to be used as a microwave undulator, however, it is interesting to note the achieved peak field levels of 46 MV/m in "normal", off the shelf waveguide. This value sets the scale on achievable circulating powers for the **second example** in table 1.

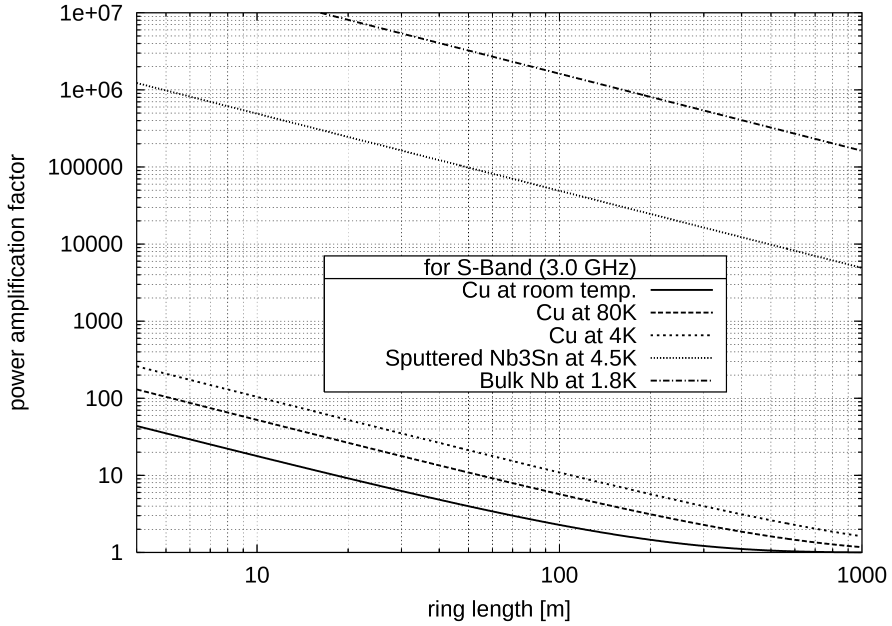

Figure 2: Theoretical power amplification factor as a function of ring length for rectangular waveguide. The operating frequency is 3 GHz for all cases and the aspect ratio of the guide cross-section is 1:4.

We consider a normalconducting 15 m long ring, ie. an undulator length of 7 m or 105 periods. From Fig. 2 a power amplification factor of 15 should be possible. For the proposed parameters only a factor 6 is required. The guide has to be manufactured with special emphasis on cleanliness and surface quality. The power source is one of the two S-Band klystrons that are still available at DESY. These klystrons were successfully operated at even higher power levels than the specified 150 MW. It should be noted, however, that the arrangement is only good for short pulses, $4\,\mu$s? long which is much shorter than the anticipated pulse length for TESLA. This microwave undulator could be practically realized on a short time scale and at relatively low cost. It could be tested in TTF as a proof of principle experiment. The gain length for the SASE FEL effect would be 1.5 m which results in a power gain of 10^3 [10]. Questions to be answered by the experiment are for instance the width and stability of the radiated spectrum as a result of the manufacturing tolerances and the RF system stability.

An interesting variant of this scheme is the superposition of the RF field with a permanent undulator field [10][11]. This would permit to realize a helical undulator with quickly switchable polarization (by changing the RF phase). Here the gain length reduces to 1 m which corresponds to 10^5 power gain.

The **third example** is a long, $L_{\rm und} = 100\,$m superconducting device. It needs 1 MW input power, a value that could probably be delivered also for long pulses (although no such klystron exists right now). The waveguide with sputtered Nb_3Sn is cheaper than bulk Nb. Furthermore the thin superconducting (sc.) layer is less sensitive in view of freezing earth magnetic field. Note the maximum magnetic surface field of 0.1 T is the same as in the TESLA L-band accelerating structures at 25 MV/m accelerating gradient. A problem with this device is that no smart idea exists so far on incorporating the necessary focusing quadrupoles into the scheme.

The **fourth example** makes use of the extremely small losses in bulk Nb at superfluid He temperatures. For a moderate ring length of 20 m or so amplification factors beyond 10^6 seem possible. This makes it feasible to drive the device with solid state amplifiers! Of course there is no such ring working right now and it requires probably considerable efforts to build one. For instance one needs a superconducting directional coupler. Another problem with this scheme is that the charge-up times are rather long for the high Q TWR, in fact longer than the pulse distance for the TESLA accelerator. Therefore the device must be operated CW with the consequence of an excessive power deposition at the 1.8 K level ($\approx$ 50 W per meter ring length in our example).

Experiments on a sc. standing wave cavity were performed in Frascati, 1989, [7]. The colleagues reached a magnetic field of 300 G with only 10 W of microwave power at 6 GHz.

The **fifth example** is a circular waveguide TWR. It demonstrates the higher equivalent field levels that can be reached in round waveguide because of the better ratio between equivalent undulator field and surface magnetic field. The frequency is chosen somewhat higher, in C-band, to reach a shorter wavelength. With only 500 W input power no klystron is needed and the odd frequency should not be a problem. Due to the higher frequency the required circulating power is significantly reduced, which is also beneficial for the cryogenic load.

waveguide type	f[GHz] Dim [mm]	P_{in}[MW] P_{c}[MW]	T[K] $R_s[\Omega]$	E_{surf}[MV/m] B_{surf}[T]	B_u[T] L_u[m]	λ_u[mm] K
SLAC TWR, rect. (WR90)	11.414 11×24	30 300	293 $27 \cdot 10^{-3}$	46 0.13	0.28 (1.7)	14 0.4
poss. S-Band exp. custom rect. guide	3.0 19×76	150 900	293 $14 \cdot 10^{-3}$	35 0.09	0.21 7	57 1.2
sc. Nb_3Sn, l. pulse custom rect. guide	3.0 19×71	1 1100	4.5 $500 \cdot 10^{-9}$	42 0.1	0.24 100	59 1.4
sc. Nb, low pow. custom rect. guide	3.0 19×71	0.001 1100	1.8 $15 \cdot 10^{-9}$	42 0.1	0.24 10	59 1.4
sc. Nb, low pow. round guide	5.3 $R = 21$	0.0005 525	1.8 $20 \cdot 10^{-9}$	37 0.1	0.34 10	44 1.5

Table 1: Parameter examples for existing or proposed TWR's.

4 Tolerances

We compute the tolerances here only for rectangular guide, for circular guide they will be similar and can easily be calculated with the described methods. Static and dynamic errors are not distinguished here.

4.1 Equivalent Field Level

The equivalent field strength in the waveguide is affected by deviations from the nominal values of 1.) the microwave power, 2.) the guide dimensions, 3.) the microwave frequency. From equation (10) we compute the following error formula:

$$\left|\frac{\Delta B_u}{B_u}\right| = 0.5\left|\frac{\Delta P}{P}\right| + 0.59\left|\frac{\Delta a}{a}\right| + 0.5\left|\frac{\Delta b}{b}\right| + 0.09\left|\frac{\Delta\omega}{\omega}\right| \tag{4}$$

The RF power can be controlled with feedback loops at the level 10^{-4}, the frequency at 10^{-8} or better. The mechanical errors of the guide dimensions are the dominant source of errors at a level of 10^{-3}.

4.2 Undulator Wavelength

From equation (2) we obtain:

$$\left|\frac{\Delta\lambda_u}{\lambda_u}\right| = \sqrt{2}\left|\frac{\Delta\omega}{\omega}\right| + (\sqrt{2}-1)\left|\frac{\Delta a}{a}\right|$$

Again the dimension error dominates at 10^{-3}.

4.3 Beam Deflection Angle and Offset

The undulator should not give the beam any effective offset or deflection angle in order to allow subsequent undulator units to be aligned precisely on the photon beam axis. With (4) the equation of motion for a beam particle in a width distorted waveguide is:

$$\begin{aligned} x''(z) &= \frac{Kk_u}{\gamma}\left(1 - 0.59\cdot\frac{\Delta a(z)}{a} - 0.5\cdot\frac{\Delta b(z)}{b}\right)\cos(k_u z) \\ K &= \frac{eB_u}{m_0 c k_u} \\ k_u &= 2\pi/\lambda_u \end{aligned} \tag{5}$$

In order to obtain the beam angle at the exit of the undulator one has to integrate the equation once over the length l_u. The undulator length, or more precise the interaction length of the beam with the electromagnetic field, should be an integer multiple of the wavelength. The first error is introduced here since the effective interaction length can probably not be adjusted to better than 1 mm. For an error of this type we find $\Delta x' = \frac{Kk_u}{\gamma}\Delta s$. For a moderate beam energy of 1 GeV and 1 mm off interaction length, other parameters from example 2 in table 1, it amounts to 70 μrad. Since the error kick happens at entrance and exit of an undulator section it could be compensated empirically with correction coils in-between the sections.

The second error comes from the width variations of the waveguide $\Delta a(z), \Delta b(z)$ along the length. Such variations are more or less random and can be considered using their statistical properties. Here we characterize the width variations by two numbers, the rms value of the variations σ_a, σ_b and a typical correlation length l_c along the longitudinal dimension. For experts: the underlying model in the calculation is an Ornstein-Uhlenbeck process [8][9]. For this process the autocorrelation function of the thickness variation is given by $\langle \Delta a(z) \Delta a(z + \Delta z) \rangle = \sigma_a^2 \exp(-|\Delta z|/l_c)$. The knowledge of the autocorrelation function is sufficient to compute the expectation value of $\langle \Delta x'^2 \rangle$ at the end of the undulator. Details are found in the Appendix. Finally we obtain:

$$\Delta x'_{\mathrm{rms}}(z = l_u) = \frac{K}{\gamma} \frac{k_u}{\sqrt{k_u^2 + 1/l_c^2}} \sqrt{\frac{l_u}{l_c}} \cdot \sqrt{0.59^2 \cdot \frac{\sigma_a^2}{a^2} + 0.5^2 \cdot \frac{\sigma_b^2}{b^2}}$$

This result has the typical scaling of a diffusion process, i.e. it grows proportional to the square root of the path length. If we assume, for example, rms width errors of $\sigma_a = 0.1\,\mathrm{mm}$, $\sigma_b = 0.05\,\mathrm{mm}$, a correlation length $l_c = 100\,\mathrm{mm}$ and an undulator length of $7\,\mathrm{m}$, the expectation value of the rms angle is $5\,\mu\mathrm{rad}$. For the beam offset we expect $\Delta x_{\mathrm{rms}} = 0.66 \cdot l_u \Delta x'_{\mathrm{rms}} \approx 23\,\mu\mathrm{m}$.

It has to be noted that this result is obtained for a flat wavelength spectrum of the pipe distortions, as it was assumed in the model. If the pipe distortions were exactly in phase with the undulator wavelength one would expect a much larger deflection of the beam. On the other hand the used simple model process exhibits rather strong variations also at short wavelength $\lambda \ll l_c$ which make the result worse. More precise model calculations can be repeated, for example, with survey data of a realistic waveguide, delivered by a 3D measuring machine.

For a normalconducting TWR it would be quite simple to correct the beam orbit with correction coils on the waveguide. However, superconducting guide shields any magnetic field and consequently it seems rather impossible to correct the orbit within an undulator section. Mechanical deformation of the guide, similar to the principle of a squeeze type phase shifter, is theoretically a possible way to add orbit deflections, but the technical difficulties are quite substantial. The most straightforward way is probably to limit the length of the sections such that no intra-undulator correction is needed.

4.4 High Q Related Errors

For the schemes with very high amplification factor (bulk Nb at 1.8K) the quality factor can be large:

$$\begin{aligned} Q_0 &\approx \frac{\omega}{4\pi\alpha c\sqrt{1 - \omega_c^2/\omega^2}} \\ &\approx 2 \cdot 10^9 \end{aligned} \tag{6}$$

Consequently the width of the resonance is very sharp, $\Delta f \approx 1.5\,\mathrm{Hz}$. It might be difficult not only to hit the resonance exactly, but also to concentrate the required RF power within this small bandwidth. Another difficulty are length changes of the resonant ring. Length changes by an amount dl have to be compensated by frequency changes of:

$$\frac{dl}{l} = -\frac{1}{1 - \omega_c^2/\omega^2} \cdot \frac{d\omega}{\omega}$$

Since the resonance width $\Delta\omega/\omega = 1/Q_0$ is rather small the ring runs out of resonance already for length changes of $dl/l \approx 2 \cdot 10^{-10}$. As far as practical experience is concerned, the frequency regulation for test measurements of TESLA cavities at critical coupling has to deal with similar tolerances. In this context one can expect difficulties with the helical undulator since the two modes can easily require different frequencies to stay in resonance, because of slightly different phase advances in the two planes [13]. Different frequencies, however, would destroy the fixed phase relationship of the two modes, which is of course required for a proper functioning of the helical undulator.

Another source of errors is the (practically unavoidable) buildup of a backward wave in the TWR which is known to be a problem for traveling wave resonators in accelerating mode [12]. The backward wave also deflects the beam and leads to orbit deviations from a straight line. The amplitude of the backward wave depends on the reflection factors in the TWR components. To estimate this effect properly one needs some practical experience, especially with sc. TWR's.

Furthermore it should be mentioned here that the RF field in the TWR has to be in a certain fixed frequency and phase relationship with the accelerating structures in the linac.

5 Discussion

Compared with a conventional undulator the microwave undulator has several advantages, but also disadvantages as listed below.

Advantages:

- Tunability: The field strength can be controlled very fast through the microwave power. Even intra train sweeps of the radiation frequency seem to be possible for the TESLA train structure.

- Tolerances: Manufacturing tolerances of the waveguide width and length are tight but not pushed to the limits. Temperature stabilization of the guide is not necessary (in case of the nc. version).

- Pipe Apertures not Critical: The aperture provided by the waveguide is significantly larger than the typical pipe apertures that are presently discussed for the conventional undulator scheme. This relaxes problems with resistive wall and rough surface wakefield effects that disturb the beam quality.

- no Radiation Damage: One of the critical issues for the conventional permanent magnet undulator is the potential danger of demagnetization of the magnet material by radiation. This is no issue for the microwave undulator.

- Simplicity: The mechanical arrangement of a microwave undulator is very simple, although one has to take into account the efforts that have to be put into the RF system.

- Short Wavelength Possible: By choosing a higher frequency one can achieve relatively short undulator wavelengths. The X-band example with WR90 waveguide gives a wavelength of $\lambda_u = 14\,\mathrm{mm}$.

Disadvantages:

- Field Strength: It is difficult to reach the same field strength as with a conventional undulator. The best performance can possibly be obtained in a round sc. guide with an equivalent field strength of 0.35 T and circular polarization. However, such a device certainly needs considerable R&D before it can be built.

- Stability: As a dynamical and pulsed device an RF system is in general less stable than a static magnet. With feedback loops it should be possible to reach the required stability, but probably never the same reliability as with a conventional undulator.

In order to push the development of the microwave undulator at DESY the next step could be to carry out the proof of principle experiment, for example setup 2 in table 1. If the results are encouraging some R&D can be started on a superconducting device. It seems that two approaches (or even a combination of them) are especially attractive: 1.) A short sc. TWR with a quality factor in a region were it could be driven by a solid state amplifier. The enormous amplification factor can be kept under control by a feedback loop. High Q related difficulties with this scheme are described in the section on tolerances. 2.) Circular superconducting waveguide excited with a helical mode. This device has the potential to reach the same power output as an 0.5 T planar undulator.

The applicability of the microwave undulator with its achievable parameters for a SASE FEL, for example in view of gain length, stability, tolerances etc. remains to be checked in detail.

6 Appendix

6.1 Rectangular Waveguides

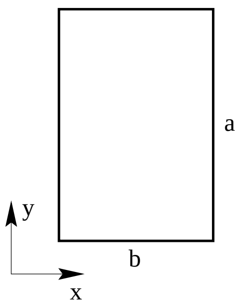

Orientation of rectangular waveguide. The ratio a/b should be at least 2 in order to provide the maximum frequency space for the fundamental mode.

6.1.1 Field Components

The nonzero field components of the TE_{10} mode, back-traveling wave, are given by:

$$\begin{aligned} E_x &= E_0 \sin(\pi y/a) \sin(\omega t + k_g z) \\ B_y &= \frac{E_0}{c}\sqrt{1-\frac{\omega_c^2}{\omega^2}} \sin(\pi y/a) \sin(\omega t + k_g z) \\ B_z &= \frac{E_0}{c}\frac{\omega_c}{\omega} \cos(\pi y/a) \cos(\omega t + k_g z) \end{aligned} \tag{7}$$

The cutoff frequency is $\omega_c = \pi c/a$. By comparing the Lorentz force on a particle at speed of light with the force in a conventional undulator we find the equivalent undulator field[1]:

[1]This relation holds for any guide cross-section.

$$
B_u = \frac{E_0}{c}\left(1+\sqrt{1-\omega_c^2/\omega^2}\right)
$$

6.1.2 Maximum Surface Field

The maximum B field on the metal surface is given by $B_{\mathrm{surf}} = \max_{y,t}(B_y^2+B_z^2)^{1/2}$. With respect to the y coordinate as well as the z coordinate we can make use of the fact that

$$
\max_s \sqrt{A^2\cos^2(s)+B^2\sin^2(s)} = \max(A,B)
$$

We find

$$
B_{\mathrm{max}} = \frac{E_0}{c}\max\left(\frac{\omega_c}{\omega}, \sqrt{1-\omega_c^2/\omega^2}\right)
$$

The minimum is achieved for choosing

$$
\frac{\omega_c}{\omega} = \frac{1}{\sqrt{2}} \approx 0.71
$$

With this choice for the operating frequency we obtain finally

$$
\begin{aligned}
B_{\mathrm{max}} &= B_u\,\frac{1}{1+\sqrt{2}} \\
B_u &\approx 2.4\cdot B_{\mathrm{max}}
\end{aligned} \tag{8}
$$

The maximum electric field is:

$$
\begin{aligned}
E_{\mathrm{max}} &= \frac{cB_u}{1+\sqrt{1-\omega_c^2/\omega^2}} \\
&\approx 0.59\cdot cB_u
\end{aligned} \tag{9}
$$

6.1.3 Microwave Power

The microwave power transported by the TE_{10} mode is computed by integrating the squared z component of the $\vec{H}$ field over the waveguide cross-section [5]:

$$
\begin{aligned}
P &= \frac{Z_0}{2}\sqrt{1-\frac{\omega_c^2}{\omega^2}}\frac{\omega^2}{\omega_c^2}\int H_z^2 dA \\
&= \frac{\pi Z_0 E_0^2}{2\mu_0^2 c^2}\sqrt{1-\frac{\omega_c^2}{\omega^2}}\,b\int_0^a dx\cos^2(\pi x/a) \\
&= \frac{abE_0^2}{4Z_0}\sqrt{1-\frac{\omega_c^2}{\omega^2}}
\end{aligned}
$$

For the equivalent undulator field we obtain finally:

$$
\begin{aligned}
B_u &= \frac{2}{c}\sqrt{\frac{Z_0 P}{ab}}\left(\left(1-\frac{\omega_c^2}{\omega^2}\right)^{-1/4}+\left(1-\frac{\omega_c^2}{\omega^2}\right)^{1/4}\right)\\
B_u[\mathrm{T}] &\approx 2.6\cdot 10^{-4}\sqrt{\frac{P\ [\mathrm{MW}]}{ab\ [\mathrm{m}^2]}}\ \ (\omega=\sqrt{2}\omega_c)\\
B_u[\mathrm{T}] &\approx 2.5\cdot 10^{-3}\ f[\mathrm{GHz}]\ \sqrt{P\ [\mathrm{MW}]}\ \ (a=4b)
\end{aligned}
\tag{10}
$$

6.1.4 Attenuation

The attenuation constant per m is given by:

$$
\alpha^{\mathrm{TE}_{10}} = \frac{R_s}{Z_0 b\sqrt{1-\omega_c^2/\omega^2}}\left(1+2\frac{b\omega_c^2}{a\omega^2}\right) \tag{11}
$$

For $a = 4b$, $\omega^2 = 2\omega_c^2$ and Copper we obtain:

$$
\alpha^{\mathrm{TE}_{10}}[\mathrm{m}^{-1}] \approx 0.72\cdot 10^{-3}(f[\mathrm{GHz}])^{3/2} \tag{12}
$$

6.2 Circular Waveguides

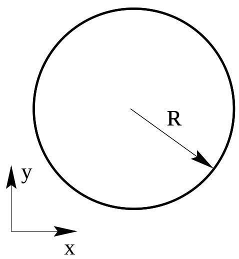

Circular waveguide.

6.2.1 Field Components

The nonzero field components of the TE_{11} mode, back-traveling wave, are given by:

$$
\begin{aligned}
E_r &= E_0\frac{R}{a'_{11}r}J_1\left(\frac{a'_{11}}{R}r\right)\cos(\phi)\sin(\omega t+k_g z)\\
E_\phi &= -E_0 J'_1\left(\frac{a'_{11}}{R}r\right)\sin(\phi)\sin(\omega t+k_g z)\\
B_r &= \frac{E_0}{c}\sqrt{1-\omega_c^2/\omega^2}J'_1\left(\frac{a'_{11}}{R}r\right)\sin(\phi)\sin(\omega t+k_g z)\\
B_\phi &= \frac{E_0}{c}\sqrt{1-\omega_c^2/\omega^2}\frac{R}{a'_{11}r}J_1\left(\frac{a'_{11}}{R}r\right)\cos(\phi)\sin(\omega t+k_g z)\\
B_z &= j\frac{E_0}{c}\frac{\omega_c}{\omega}J_1\left(\frac{a'_{11}}{R}r\right)\sin(\phi)\cos(\omega t+k_g z)
\end{aligned}
\tag{13}
$$

Here R is the radius of the waveguide, $a'_{11} = 1.841$ is the first zero of the first derivative of the J_1 Besselfunction. The constant $J_1(a'_{11}) = 0.5818$ is needed for numerical evaluations. The cutoff frequency in the circular case is $\omega_c = a'_{11}c/R$.

The field is scaled such that on the pipe axis the peak fields are:

$$\begin{aligned}\hat{E}_x(r=0) &= E_0 \\ \hat{B}_y(r=0) &= \frac{E_0}{c}\sqrt{1-\omega_c^2/\omega^2}\end{aligned}$$

In the vicinity of the pipe center the field is practically equal to the TE_{10} mode in rectangular guide. The equivalent undulator field is again

$$B_u = \frac{E_0}{c}\left(1+\sqrt{1-\omega_c^2/\omega^2}\right)$$

6.2.2 Maximum Surface Field

The B field on the metal surface is given by $B_{\mathrm{surf}} = (B_\phi^2 + B_z^2)^{1/2}|_{r=R}$.

With the same argumentation as for the rectangular waveguide we find

$$B_{\max} = \frac{E_0}{c} J_1(a'_{11}) \max\left(\frac{\omega_c}{\omega}, \sqrt{1-\omega_c^2/\omega^2}/a'_{11}\right)$$

The optimum is achieved for choosing

$$\frac{\omega_c}{\omega} = \frac{1}{\sqrt{1+a'^2_{11}}} \approx 0.477$$

With this choice for the operating frequency we obtain

$$\begin{aligned}B_{\max} &= B_u \frac{J_1(a'_{11})}{a'_{11} + \sqrt{1+a'^2_{11}}} \\ B_u &\approx 6.8 \cdot B_{\max}\end{aligned}$$

However, it turns out that ω should not be chosen higher than $1.307 \cdot \omega_c$ in order to avoid excitation of the next higher mode. For a choice $\omega_c/\omega = 4/5$ we find:

$$\begin{aligned}B_{\max} &= B_u \frac{J_1(a'_{11})}{2} \\ B_u &\approx 3.4 \cdot B_{\max} \qquad (14)\end{aligned}$$

The maximum electric field is given by (same choice of frequency):

$$\begin{aligned}E_{\max} &= E_0 J_1(a'_{11})/a'_{11} \\ E_{\max} &\approx 0.364 \cdot cB_u \qquad (15)\end{aligned}$$

6.2.3 Microwave Power

Again the microwave power of the TE_{11} mode is computed by integrating the squared z component of the H field over the waveguide cross-section:

$$
\begin{aligned}
P &= \frac{Z_0}{2}\sqrt{1-\frac{\omega_c^2}{\omega^2}}\frac{\omega^2}{\omega_c^2}\int H_z^2 dA \\
&= \frac{\pi Z_0 E_0^2}{2\mu_0^2 c^2}\sqrt{1-\frac{\omega_c^2}{\omega^2}}\int_0^R r J_1\left(\frac{a'_{11}}{R}r\right) dr \\
&= \frac{\pi E_0^2 R^2}{4 Z_0}\sqrt{1-\frac{\omega_c^2}{\omega^2}}\left(1-\frac{1}{a'^2_{11}}\right) J_1^2(a'_{11})
\end{aligned}
$$

Finally we obtain for the equivalent undulator field as a function of microwave power and pipe diameter:

$$
\begin{aligned}
B_u &= \frac{2}{cRJ_1(a'_{11})}\sqrt{\frac{Z_0 P}{\pi(1-1/a'^2_{11})}}\left(\left(1-\frac{\omega_c^2}{\omega^2}\right)^{-1/4}+\left(1-\frac{\omega_c^2}{\omega^2}\right)^{1/4}\right) \\
B_u[\mathrm{T}] &\approx 3.0\cdot 10^{-4}\,\frac{\sqrt{P\ [\mathrm{MW}]}}{R\ [\mathrm{m}]} \quad (\omega = 1.25\cdot\omega_c) \\
&\approx 2.8\cdot 10^{-3}\ f[\mathrm{GHz}]\sqrt{P\ [\mathrm{MW}]} \qquad (16)
\end{aligned}
$$

6.2.4 Attenuation

The attenuation per m is given by:

$$
\alpha^{\mathrm{TE}_{11}} = \frac{R_s}{Z_0 R\sqrt{1-\omega_c^2/\omega^2}}\left(\frac{\omega_c^2}{\omega^2}-\frac{1}{1-a'^2_{11}}\right) \qquad (17)
$$

for $\omega_c/\omega = 4/5$ and Copper we obtain:

$$
\alpha^{\mathrm{TE}_{11}}[\mathrm{m}^{-1}] \approx 0.35\cdot 10^{-3}(f[GHz])^{3/2} \qquad (18)
$$

6.3 Beam Orbit for a Width Distorted Waveguide

The equation of motion (5) is the starting point for our estimate of the expectation values of the rms angular deviation and rms beam offset. For simplicity we include only the variation of the guide width a:

$$
\begin{aligned}
\left\langle \Delta x'^2(z)\right\rangle &= \frac{K^2 k_u^2}{\gamma^2 a^2}\int_{t=0}^{z}\int_{s=0}^{z} dt\ ds\ \langle\Delta a(t)\Delta a(s)\rangle\cos(k_u t)\cos(k_u s) \\
&= \frac{K^2 k_u^2}{\gamma^2 a^2}\int_{t=0}^{z}\int_{s=0}^{z} dt\ ds\ \sigma_a^2\exp\left(-\frac{|t-s|}{l_c}\right)\cos(k_u t)\cos(k_u s) \\
&\approx \frac{K^2\sigma_a^2}{\gamma^2 a^2}\frac{k_u^2}{k_u^2+1/l_c^2}\ \frac{z}{l_c} \qquad (19)
\end{aligned}
$$

By simple integration of $\Delta x'_{\mathrm{rms}}(z)$ we obtain for the rms beam offset: $\Delta x_{\mathrm{rms}}(z) = 2/3\ z\ \Delta x'_{\mathrm{rms}}(z)$. Both results were confirmed by numerical simulations (Fig. 3).

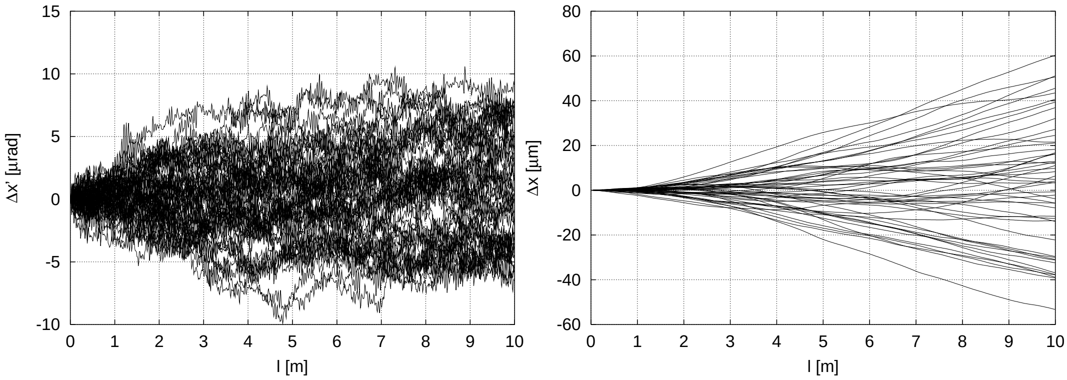

Figure 3: Model calculations for beam angle (left plot) and beam offset along the microwave undulator for 50 different seeds of a width distorted waveguide. The parameters are: $\sigma_a = 100\,\mu\mathrm{m}$, $\sigma_b = 0$, $l_c = 100\,\mathrm{mm}$, and those of example 2 in table 1.

References

[1] T. Shintake et al., Development of Microwave Undulator, Jap. Journal of Appl. Phys., Vol. 22, 844-851 (1983)

[2] K. Batchelor, Microwave Undulator, Linac Accelerator Conference Proceedings, Stanford (1986)

[3] H. Padamse, J. Knobloch, T. Hays, RF Superconductivity for Accelerators (1998)

[4] C. Benvenuti (CERN) reported at DESY in 7/00 on measurements of an L-band cavity of TESLA shape with a sputtered Nb_3Sn surface. The value for R_s was estimated from a measured Q-value of $3 \cdot 10^8$ at $E_{\mathrm{acc}} = 20\,\mathrm{MeV/m}$.

[5] J. D. Jackson, Classical Electrodynamics, Wiley & Sons (1975)

[6] X. Xu et al., RF Breakdown Studies in X-Band Klystron Cavities, SLAC-Pub 7505 (1997)

[7] R. Boni et al., Superconducting Microwave Undulator, Rev. Sci. Instrum. 60(7), July 1989, 1805-1808

[8] C.W. Gardiner, Handbook of Stochastic Methods, Springer (1985)

[9] H. Mais, private communication in (2000)

[10] J. Schneidmiller, private communication (2000)

[11] T. Shintake, RF Insertion Devices, Workshop on 4'th Generation SR Sources, SLAC (1992)

[12] P. Wilson, Application of Traveling Wave Resonantors to Superconducting Linear Accelators, PAC (1971)

[13] M. Dohlus, private communication in (2000)